OF **COLLEGE**

ENGINEERING

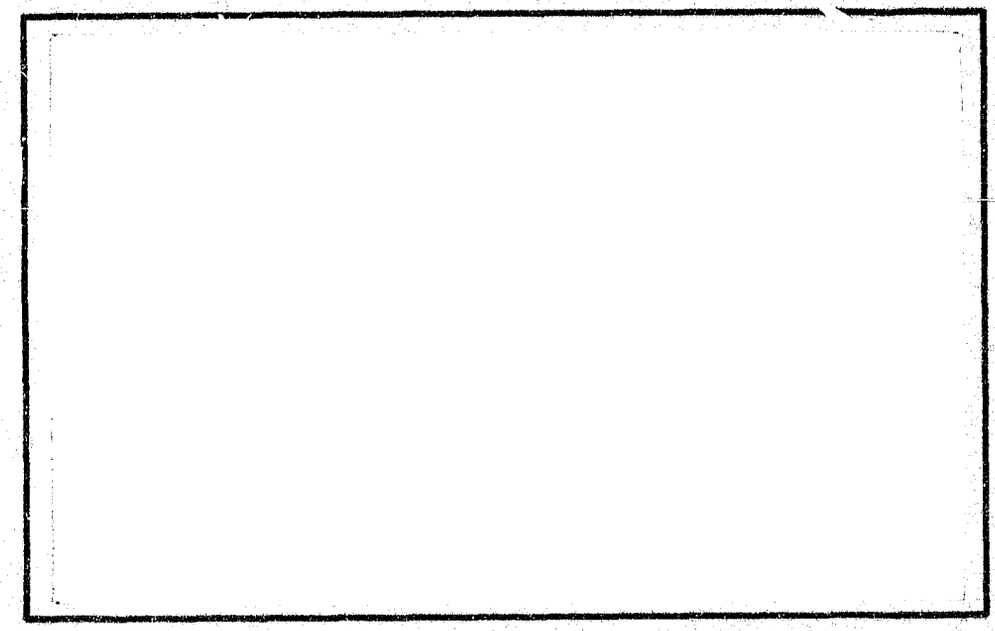

VIRGINIA POLYTECHNIC INSTITUTE AND STATE UNIVERSITY

BLACKSBURG, VIRGINIA

COMPOSITE MATERIALS RESEARCH AND EDUCATION

March 20, 1981

Notice! Table 2 was inadvertently left out of the VPI-E-81-2 report you recently received entitled "On the Relationship Between Engineering Properties and Delamination of Composite Laminates." The table is enclosed for completeness. Please insert it after Table 1.

THE NASA-VIRGINIA TECH COMPOSITES PROGRAM

National Aeronautics & Space Administration
Langley Research Center
Hampton, Virginia 23665

Virginia Polytechnic Institute
and State University
Phone 703-961-5372

reply to The NASA-Virginia Tech Composites Program
Dept of Engineering Science & Mechanics
Virginia Tech
Blacksburg, Virginia 24061

ON THE RELATIONSHIP BETWEEN ENGINEERING PROPERTIES AND DELAMINATION OF COMPOSITE LAMINATES

C T. Herakovich

Virginia Polytechnic Institute and State University
Blacksburg, Virginia

February 1981

ON THE RELATIONSHIP BETWEEN ENGINEERING PROPERTIES AND DELAMINATION OF COMPOSITE LAMINATES

by

CARL T. HERAKOVICH*

ABSTRACT :

The influence of the coefficient of mutual influence, poisson's ratio and coefficients of thermal and moisture expansion on delamination is studied. Engineering theoriesare compared to finite element and experimental results. It is shown that the mismatch in coefficient of mutual influence can have a strong influence on delamination with fiber angles in the 10°-15° range being critical for adjacent (±θ) layer combinations. The mismatch in coefficient of mutual influence is reduced by a factor of two and the interlaminar shear stress τ_{zx} is reduced significantly when the ±θ layers are interspersed between 0° and 90° layers. It is shown how the results can be used for design of composite laminates.

---

* *Professor of Engineering Science & Mechanics, Virginia Polytechnic Institue & State University, Blacksburg, Virginia, 24061, U.S.A.*

on Sabbatical at :

Ecole Polytechnique, Laboratoire de Mécanique des Solides, 91128 Palaiseau Cedex.

INTRODUCTION

The interlaminar stresses in the boundary layer along the free edges of a laminated composite play an important role in the initiation of damage at the free edge. Delamination between layers is a direct result of these interlaminar stresses. While delamination is important to the overall structural performance of laminates under tensile loading, it is critical for compression and shear loading where stability is a major concern.

Following the initial work of Pipes and Pagano [1], numerous investigators have studied the problem of free edge effects in laminated composites. However, a systematic discussion of the fundamental relationships between the engineering properties of the individual layers and edge effects has apparently never been presented. This paper will attempt to at least partially fill this gap in the literature.

BASIC CONSIDERATIONS

Mechanical loading :

The fundamental reason for the presence of interlaminar stresses in laminated composites is the existence of a mismatch in engineering properties between layers. For the purpose of discussion we consider here the special case of a balanced, symmetric coupon under axial loading in the x direction (Fig. 1). The two most important lamina properties for this problem are poisson's ratio

$$(1)\quad \nu_{xy} = \frac{-\varepsilon_y}{\varepsilon_x} = \frac{-\overline{S}_{12}}{\overline{S}_{11}} = \frac{-\left[(n^4+m^4)\ S_{12} + n^2\ m^2\ (S_{11} + S_{22} - S_{66})\right]}{\left[m^4\ S_{11} + m^2\ n^2\ (2\ S_{12} + S_{66}) + n^4\ S_{22}\right]}\ ,$$

and the coefficient of mutual influence

$$(2)\quad \eta_{xy,x} = \frac{\gamma_{xy}}{\varepsilon_x} = \frac{\overline{S}_{16}}{\overline{S}_{11}} = \frac{\left[n\ m^3(2\ S_{11} - 2\ S_{12} - S_{16}) + m\ n^3\ (2\ S_{12} - 2\ S_{22} + S_{66})\right]}{\left[m^4\ S_{11} + m^2\ n^2\ (2\ S_{12} + S_{66}) + n^4\ S_{22}\right]}$$

where S_{ij} and $\overline{S}_{ij}$ correspond to the compliance coefficients in material principal and global coordinates, respectively, m and n are the $\cos\theta$ and $\sin\theta$, respectively, and θ is the angle of fiber orientation measured from the axis of the coupon. Equations *(1)* and *(2)* are plotted in Fig. 2 for properties typical of T300/5208 graphite/epoxy. It is noted that $\eta_{xy,x}$ is an odd function of θ with a maximum value at $\theta = 11{,}5°$ whereas ν_{xy} is even in θ with a maximum value at $\theta = 22°$.

If there is no mismatch of ν_{xy} or $\eta_{xy,x}$ between layers, there are no interlaminar stresses regardless of the mismatch in elastic and shear moduli. The mismatch of poisson's ratio between adjacent layers gives rise to dissimilar lateral strains ε_y in free (unbonded) layers, but results in identical strains at the layer interfaces with accompanying interlaminar stresses σ_y and τ_{yz} in perfectly bonded laminates. Likewise, the

$\eta_{xy,x}$ mismatch gives rise to nonzero interlaminar shear stresses τ_{zx} in bonded laminates. The magnitude of the interlaminar stresses is related to the magnitude of the mismatch in ν_{xy} and $\eta_{xy,x}$, the elastic and shear moduli and the stacking sequence. The stacking sequence plays an important role in that is establishes the moment associated with the σ_y stresses. This moment is equilibrated by the interlaminar σ_z distribution (Fig. 1).

In order to demonstrate the fundamental relationship between engineering properties and the interlaminar stresses, we consider three special classes of adjacent laminae : ($+\theta/-\theta$), ($\theta/0$), and ($\theta/90$). The properties of greatest interest are the mismatch between adjacent layers, $\delta\nu_{xy}$ and $\delta\eta_{xy,x}$ with

$$|\delta\nu_{xy}| = |\nu_{xy}(\theta_2) - \nu_{xy}(\theta_1)| \tag{3}$$

$$|\delta\eta_{xy,x}| = |\eta_{xy,x}(\theta_2) - \eta_{xy,x}(\theta_1)| \tag{4}$$

where θ_1 and θ_2 correspond to the fiber orientations of adjacent layers. Interlaminar stresses will be largest when the mismatch is maximum (all other things being equal).

Fig. 3 shows plots of $|\delta\nu_{xy}|$ and $|\delta\eta_{xy,x}|$ as a function of θ for the three special cases under consideration. The largest mismatch is observed to be $|\delta\eta_{xy,x}| = 4.34$ for the (+ 11.5/-11.5) combination. The curve exhibists a steep gradient in the vicinity of the critical value $\theta = 11.5°$. The magnitude of $\delta\eta_{xy,x}$ for the $(+\theta/-\theta)$ combination is exactly double that for the $(\theta/0)$ and $(\theta/90)$ combinations. This is because $\eta_{xy,x}$ is an odd function of θ and $\eta_{xy,x} = 0$ for $\theta = 0°$ and $\theta = 90°$. There is no mismatch in ν_{xy} for the $(+\theta/-\theta)$ combination as ν_{xy} is an even function of θ.

The maximum value of $|\delta\nu_{xy}|$ is much smaller than $|\delta\eta_{xy,x}|$ for all three laminae combinations. The worse case for $\delta\nu_{xy}$ is the $(\theta/90)$ combination with $|\delta\nu_{xy}| = 0.34$ at $\theta = 22°$. Thus, the maximum value of $|\delta\eta_{xy,x}|$ is more than ten times the maximum $|\delta\nu_{xy}|$. Since the interlaminar normal

and shear strengths are of the same order of magnitude, initiation of delamination is much more sensitive to the mismatch in coefficients of mutual influence than the mismatch is poisson's ratio. (as will be shown later, this large difference in mismatch can be partially or totally offset by the influence of stacking sequence on the magnitude of σ_z).

Close examination of Fig. 3 shows that $|\delta\eta_{xy,x}|$ is significantly larger than $|\delta\upsilon_{xy}|$ for almost the entire range of fiber angles for all three laminae combinations, the exception being as the (0/90) combination (with $\delta\eta_{xy,x} = 0$) is approached. The zero value of $\delta\eta_{xy,x}$ and the near maximum value of $\delta\nu_{xy}$ for the (0/90) combination is consistent with the rather well-know numerical result that τ_{zx} is zero in crossply laminates and delamination is solely due to interlaminar normal stresses.

Thermal and Moisture Effects

The mismatch of the coefficients of thermal and hygroscopic expansion produce edge effects similar to those due to mechanical loading [2]. The formulation of both problems is identical and hence we consider only the thermal problem for the purpose of illustration. The free thermal expansions for a uniform, unit temperature change of an unbonded lamina are

$$(5) \qquad \begin{Bmatrix} \varepsilon_x^T \\ \varepsilon_y^T \\ \gamma_{xy}^T \end{Bmatrix} = \begin{Bmatrix} m^2 \alpha_1 + n^2 \alpha_2 \\ n^2 \alpha_1 + m^2 \alpha_2 \\ 2\, m\, n\, (\alpha_1 - \alpha_2) \end{Bmatrix}$$

and the mismatch in strains of interest at the free edge can be expressed

$$(6) \quad \delta \varepsilon_y^T = \varepsilon_y^T(2) - \varepsilon_y^T(1) = (\alpha_2 - \alpha_1)\ (\cos^2 \theta_2 - \cos^2 \theta_1)$$

$$(7) \quad \delta \gamma_{xy}^T = \gamma_{xy}^T(2) - \gamma_{xy}^T(1) = (\alpha_2 - \alpha_1)\ (\sin 2\theta_1 - \sin 2\theta_2) \quad .$$

In the above, α's are coefficient of thermal expansion, subscripts x and y refer to global coordinates, and the superscript T indicates thermal effects.

Application of eqns. *(6.7)* for the three laminae combinations under consideration gives the following results :

- $(\pm\theta)$ Combination :

$$(8) \qquad \begin{aligned} \delta\varepsilon_y^T &= 0 \\ \delta\gamma_{xy}^T &= (\alpha_2 - \alpha_1)\ (2 \sin 2\theta) \\ |\delta\gamma_{xy}^T|_{max} &= 2\ (\alpha_2 - \alpha_1) \quad \text{at} \quad \theta = 45^\circ \quad . \end{aligned}$$

- (θ/O) combination :

$$\delta\varepsilon_y^T = (\alpha_2 - \alpha_1)\ (\sin^2\theta)$$

$$|\delta\varepsilon_y^T|_{max} = (\alpha_2 - \alpha_1) \quad \text{at} \quad \theta = 90°$$

(9)

$$\delta\gamma_{xy}^T = (\alpha_2 - \alpha_1)\ (\sin 2\theta)$$

$$|\delta\gamma_{xy}^T|_{max} = (\alpha_2 - \alpha_1) \quad \text{at} \quad \theta = 45° \ .$$

- (O/90) Combination :

$$\delta\varepsilon_y^T = (\alpha_2 - \alpha_1)\ (-\cos^2\theta)$$

$$|\delta\varepsilon_y^T|_{max} = (\alpha_2 - \alpha_1) \quad \text{at} \quad \theta = O°$$

(10)

$$|\delta\gamma_{xy}^T| = (\alpha_2 - \alpha_1)\ (\sin 2\theta)$$

$$|\delta\gamma_{xy}^T|_{max} = (\alpha_2 - \alpha_1) \quad \text{at} \quad \theta = 45° \ .$$

It is evident from the above that the worse case is $\delta\gamma_{xy}^T$ for the ($\pm\theta$) combination with $\theta = 45°$. The magnitude of $\delta\gamma_{xy}^T$ for the ($\pm\theta$) combination is twice that of the others, as it was for $\delta\eta_{xy,x}$; however, the critical angle has shifted from 11.5° to 45°. The mismatch $\delta\varepsilon_y^T$ is zero for the ($\pm\theta$) combination, as it was for $\delta\nu_{xy}$, but the maximum mismatch for the other two layer configurations both correspond to the (0/90) case unlike $\delta\nu_{xy}$ where the maximum mismatch occurred at $\theta = 22°$. It is also noted that the maximum $\delta\gamma_{xy}^T$ is only double that of the maximum $\delta\varepsilon_y^T$ compared to a factor of more than ten between $|\delta\eta_{xy,x}|_{max}$ and $|\delta\nu_{xy}|_{max}$. Also, the variations in thermal strain mismatch as a function of θ are smooth trigonometric functions and do not exhibit the sharp rise to a peak value as does $\delta\eta_{xy,x}$ in Fig. 3.

Since composites are cured at an elevated temperature thermal stresses are always present. For a negative change in temperature (as during cure) the thermal shear strains γ^{T}_{xy} have the opposite sign as those due to tensile loading and hence the effects tend to offset, as well as shift the critical angle. The thermal and mechanical effects would, of course, be additive for compressive loading. The combination of thermal and mechanical loading effects on $\delta\varepsilon_y$ is additive for tensile loading and offsetting for compressive loading.

NUMERICAL RESULTS FOR $[\pm\theta]_s$ LAMINATES

The discussion in the previous section is based upon somewhat heuristic arguments. Fig. 4 shows finite element results for the influence of fiber orientation on the value of the interlaminar shear stress τ_{zx} at the intersection of the interface and the free edge in $[\pm\theta]_s$ laminates [3]. The nondimensionalized stresses in the figure correspond to the maximum stress for each laminate configuration. The results were obtained for selected fiber angles of T300/5208 graphite/epoxy. The curve clearly shows a peak value at $\theta = 15°$, close to the value of 11.5° for the maximum $|\delta\eta_{xy,x}|$ and there is a distinct similarity between the distribution of $|\delta\eta_{xy,x}|$ in Fig. 3 and τ_{zx} in Fig. 4.

A failure analysis for the $[\pm\theta]_s$ laminates was performed using the finite element stress results and the Tsai-Wu tensor polynomial failure criterion [4] . Figure 5 shows the variation of the maximum value of the tensor polynomial in these laminates as a function of a fiber orientation. Again, there is a distinct peak value at $\theta = 15°$. Examination of the individual terms of the polynomial clearly indicated a dominate influence of τ_{zx} for this critical fiber orientation. Thus, there is numerical support for the heuristic arguments of the previous section.

EXPERIMENTAL RESULTS FOR $[\pm\theta]_s$ LAMINATES

The mode of failure at the free edge of $[\pm\theta]_s$ Celion 6000/PMR-15 graphite/epoxy laminates was determined in reference [5] using the edge replicating technique [6]. Figs 6-8 show replicas of the edge damage for selected laminates. The mode of damage is delamination for $[\pm 10]_s$ and $[\pm 30]_s$ laminates, but shifts to transverse cracking for the $[\pm 60]_s$ laminate. These results give experimental support for the dominate influence of $\eta_{xy,x}$ in the 10°-30° range of fiber orientations for $[\pm\theta]_s$ laminates.

LAMINATE DESIGN

The results in Fig. 3 can serve as a guide to the designer in choosing fiber orientations and stacking sequence in applications with free edges. Consider the case of the quasi-isotropic laminate with fiber orientations of 0°, 90°, + 45° and -45°. An often asked question is : what is the optimum stacking sequence ? The curves in Fig. 3 suggest that the interlaminar shear stresses τ_{zx} will be significantly lower if the + 45° and - 45° layers are separated by a 0° or 90° layer.

Of the twenty-four possible combinations of layers in this laminate, only twelve are distinct because of the interchangeability of the + 45° and - 45° layers. Of these twelve, there are six possibilities with adjacent ± 45° layers and six with ± 45° layers interspersed between 0° and 90° layers. These twelve laminates are depicted in Tables 1 & 2 along with the magnitude and direction of the σ_y stresses for tensile loading ε_x=0,5%. Also indicated in the Tables is pertinent information as to the magnitude and direction of the equilibrating moment at each interface, and the maximum σ_z and τ_{zx} stresses determined from a finite element stress analysis.

A hierarchy of lamiantes for resistance to delamination can be established through consideration of the magnitude of $\delta\eta_{xy,x}$ and the magnitude and direction of the interface moment. The hierarchy given in the Tables is based upon the following guidelines listed in order of senverity :

1. avoid adjacent ± 45° layers
2. select the most negative or smallest positive interface moment

The analysis indicates that the $[90/45/0\text{-}45]_s$ laminate provides the greatest resistance to delamination for tensile loading. This laminate has the ± 45° layers interspersed and the interface moment is negative throughout. In contrast, the $[45/0/\text{-}45/90]_s$ laminate is the worst case of the six with interspersed ± 45° layers, because the interface moment is always positive and of maximum magnitude.

The hierarchy presented in the tables does not include the influence of combined stress states nor the effects of residual thermal or hygroscopic stresses. Thus it is expected that experimental results may indicate some reordering of the list. A linear elastic finite element stress analysis of the twelve possible laminate configurations was conducted to obtain approximate elastic stress distributions. The magnitude and location of the maximum values of σ_z and τ_{zx} are presented in the tables along with a strength hierarchy based upon the following guidelines :

1. minimize $|\tau_{zx}|$
2. minimize σ_z .

The finite element results clearly show the advantages to be gained with interspersed ± 45° layers. All six laminates with interspersed ± 45° layers have lower interlaminar shear stresses than those with adjacent ± 45° layers. The magnitude of the interlaminar shear stress ranges from a low of 5.8 KSI (39.9 MPa) for the $[45/0/90/\text{-}45]_s$ laminate to a high of 9.2 KSI (63.8 MPa) for the $[90/45/\text{-}45/0]_s$ laminate, a sixty percent difference. The range of σ_z stresses for interspersed ± 45° layers is smaller than that for the adjacent layer configuration indicating a more efficient design with interspersed ± 45's in the presence of alternating

positive/negative loads. The hierarchy based upon the finite element stress results is the same as that based upon the engineering or heuristic approach.

It is interesting to note that the great majority of experimental results reported in the literature for delamination studies of quasi-isotropic laminates have been obtained from specimens with adjacent ± 45° layers [6-8]. The only exception known to the author is that of reference 9 where it was shown that the strain at first delamination in a $[\pm 45/0/90]_s$ laminate was approximately half the strain at first delamination in a $[0/45/90/-45]_s$ laminate. The $[\pm 45/0/90]_s$ specimen delaminated along the midplane due to high interlaminar normal stresses and the $[0/45/90/-45]_s$ specimen delaminated in the 90° layer, apparently due to combined σ_z and τ_{zx} effects.

Further evidence of the importance of adjacent ± 45° layers on failure of quasi-isotropic laminates were presented in reference [6]. The final fracture patterns $[0/\pm 45/90]_s$ and $[0/90/\pm 45]_s$ graphite-epoxy laminates exhibited extensive delamination along the ± 45° interface of both laminates even though the interlaminar normal stress is compressive along this interface in the $[0/90/\pm 45]_s$. The finite element results of this study indicated very high interlaminar shear stresses for this interface (Table 2).

DISCUSSION

Delamination has been studied with an emphasis on straight coupons under tensile loading. It has been pointed out that adjacent ± θ layers leads to high interlaminar shear stresses and that interlaminar normal stresses are very dependent on stacking sequence. Since shear failure is independent of loading direction, adjacent ± θ layers should generally be avoided. There are a limited number of situations where the free edges are always parallel to the loading axis and the direction of loading is know to be constant. In such situations there may be justification for adjacent ± θ layers in order to optimize the negative interlaminar normal stress ; however this can only be accomplished at the expense of significantly higher interlaminar shear stress (Table 2). In many application the loading direction will change during service and free edges are often present in the form of holes and cutouts eliminating the condition of a single known direction of loading. Interspersed ± θ layers are preferred in such applications as interlaminar shear stresses are reduced as are the extremes of interlaminar normal stresses. An example has been given as to how these results can be used systematically in design to minimize the possibility of delamination.

CONCLUSIONS

It has been shown that there is a fundamental relationship between delamination and the "mismatch" of engineering properties between adjacent layers of laminated composites. Interlaminar shear stresses are primarily a function of the mismatch in coefficients of mutual influence which can be as much as ten times greater than the mismatch in poisson's ratio. The mismatch in coefficients of mutual influence has a high peak value in the 10°-15° fiber range for ± θ laminae combinations. This mismiatch is reduced by a factor of two when the ± θ layers are interspersed between 0° and 90° layers. Interspersed ± θ are recommended for more efficient design.

ACKNOWLEDGEMENT

This work was supported by NASA contract NAS 1-15080, task n° 14, and the NASA-Virginia Tech. Composites Program, NASA CA NCCI-15. Portions of the work were completed while the author was on Sabbatical at Ecole Polytechnique, Palaiseau, France, with support from Society National Industrial Aerospatial (SNIAS).

REFERENCES

[1] PIPES R.B. and PAGANO N.J., "*Interlaminar Stresses in Composite Laminates Under Uniform Axial Extension*", J. Composite Materials, vol. 4, 1970, pp. 538-548.

[2] FARLEY G.L. and HERAKOVICH C.T., "*Influence of Two-Dimensional Hygrothermal Gradients on Interlaminar Stresses Near Free Edges*", Advanced Composite Materials-Environmental Effects, ASTM STP 658 J.R. Vinson, Ed., Am. Soc. Testing & Materials 1978, pp. 143-159.

[3] HERAKOVICH C.T., NAGARKAR A. and O'BRIEN D.A., "*Failure Analysis of Composite Laminates with Free Edges*", Modern Developments in Composite Materials and Structures, J.R. Vinson Ed., ASME 1979.

[4] TSAI S.W. and WU E.M., "*A General Theory of Strength for Anisotropic Materials*", J. Comp. Materials, vol. 5, 1971, pp. 58-80.

[5] KLANG E. and HERAKOVICH C.T., (to be published).

[6] STALNAKER D.O. and STINCHCOMB W.W., "*Load History Edge Damage Studies in Two Quasi-Isotropic Graphite Epoxy Laminates*", Composites Materials, Testing and Design, ASTM, STP 674, pp. 620-641, 1979.

[7] KRIZ R.D., STINCHCOMB W.W., TENNEY D.R., "*Effects of Moisture, Residual Thermal Curing Stresses & Mechanical Load on the Damage Development in Quasi-Isotropic Laminates*", VPI-E-80-5, Virginia Polytechnic Institute, Feb. 1980.

[8] CROSSMAN F.W., "*Analysis of Free Edge Induced Failure of Composite Laminates*", Fracture of Composite Materials (Editors, Sih & Tamuzs), Sijthoff and Noordhoff, 1979.

[9] MILLSJ.S., HERAKOVICH C.T., DAVIS J.G. Jr., "*Transverse Microcracking in Celion 6000/PMR-15 Graphite-Polyimide*", VPI-E-79-35, Virginia Polytechnic Institute, Dec. 1979.

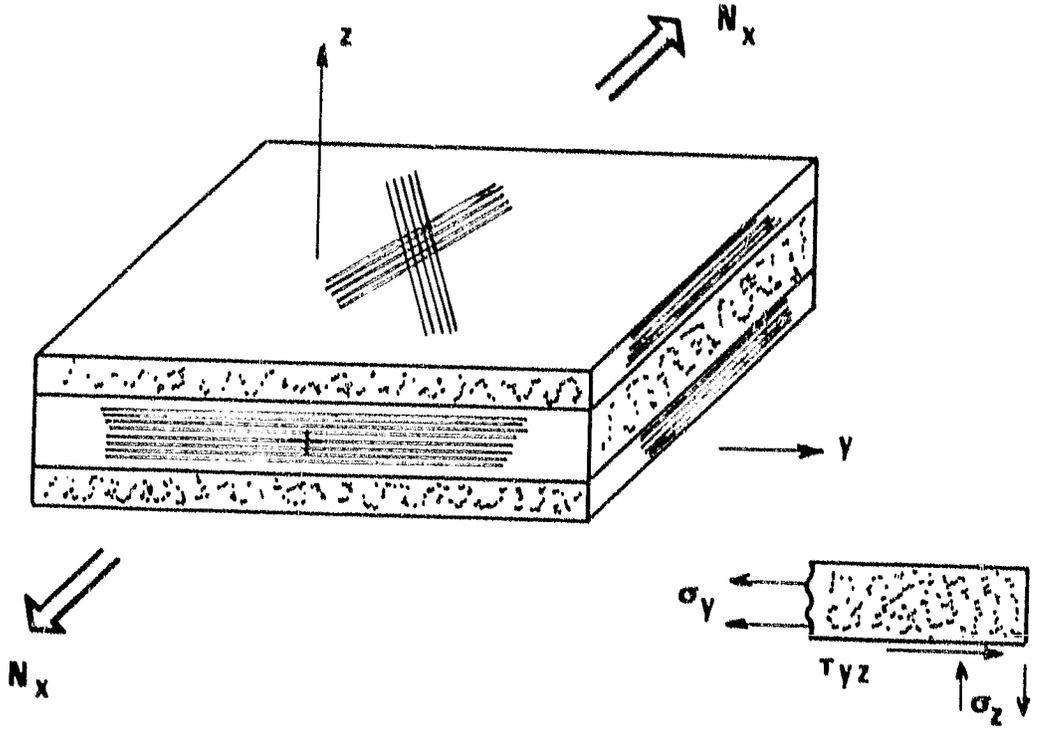

equilibrium free body diagram

Figure 1 - Balanced, symmetric coupon under axial load

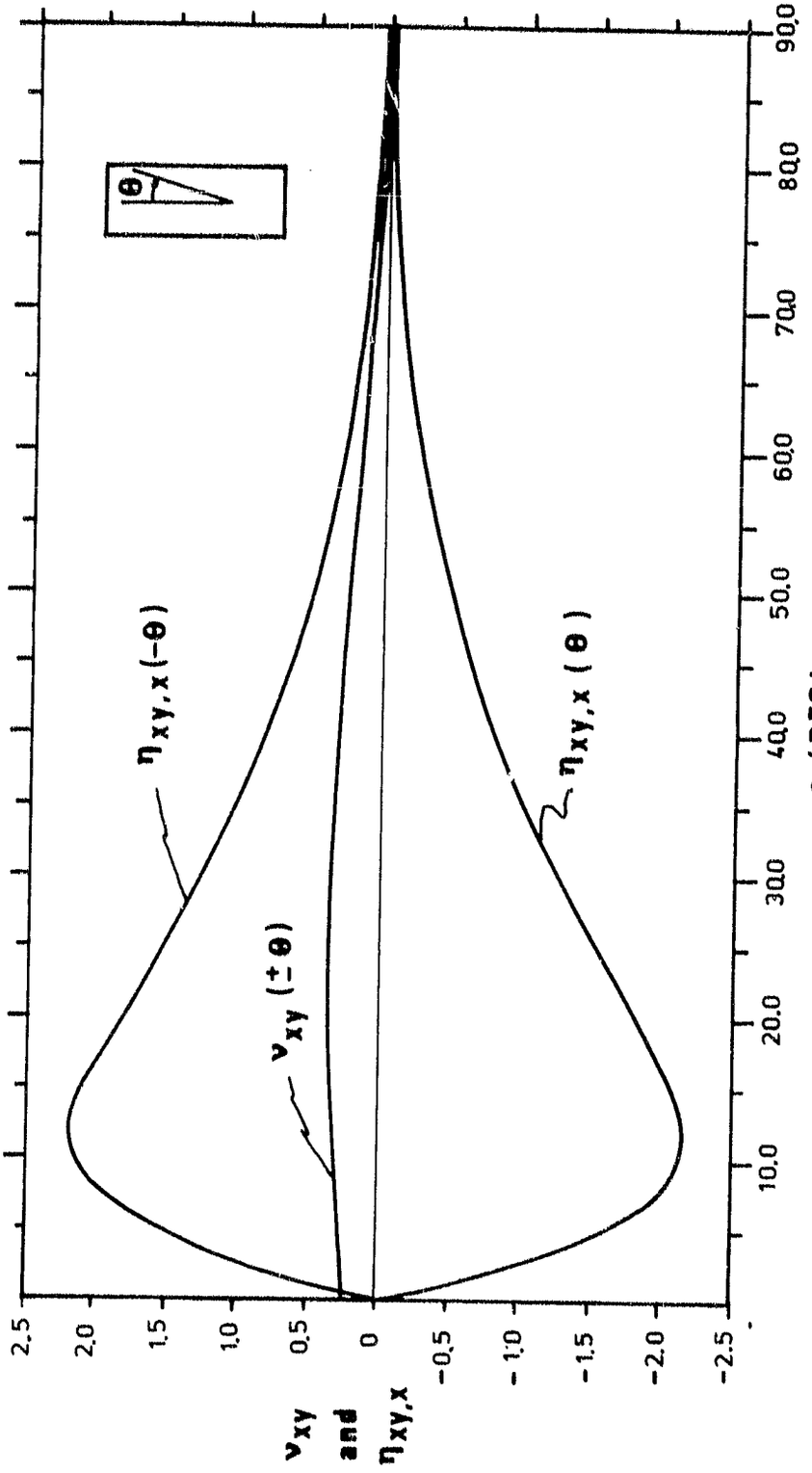

Figure 2 - ν_{xy} and $\eta_{xy,x}$ for unidirectional T300/5208 Graphite-Epoxy

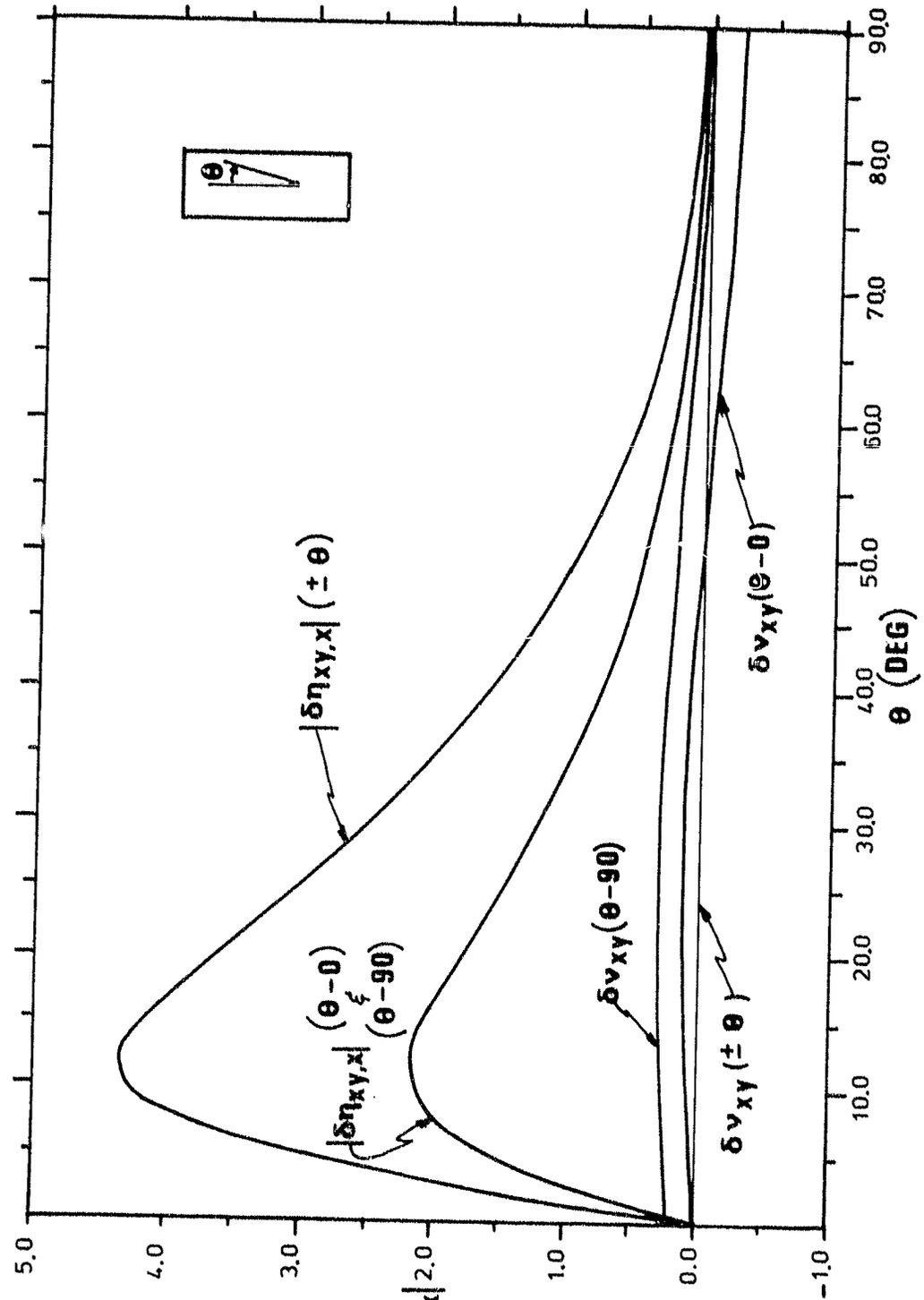

Figure 3 - Mismatch of Possion's ratio and coefficient of mutual influence for T300/5208 Graphite-Epoxy

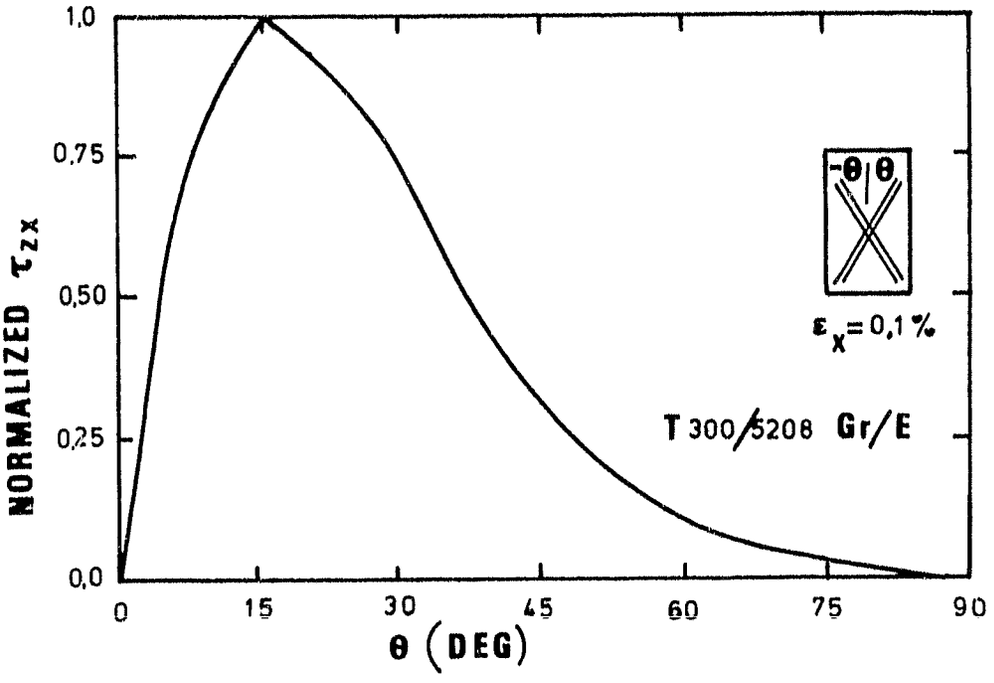

Figure 4 - Maximum τ_{zx} for $[\pm \theta]_s$ laminates

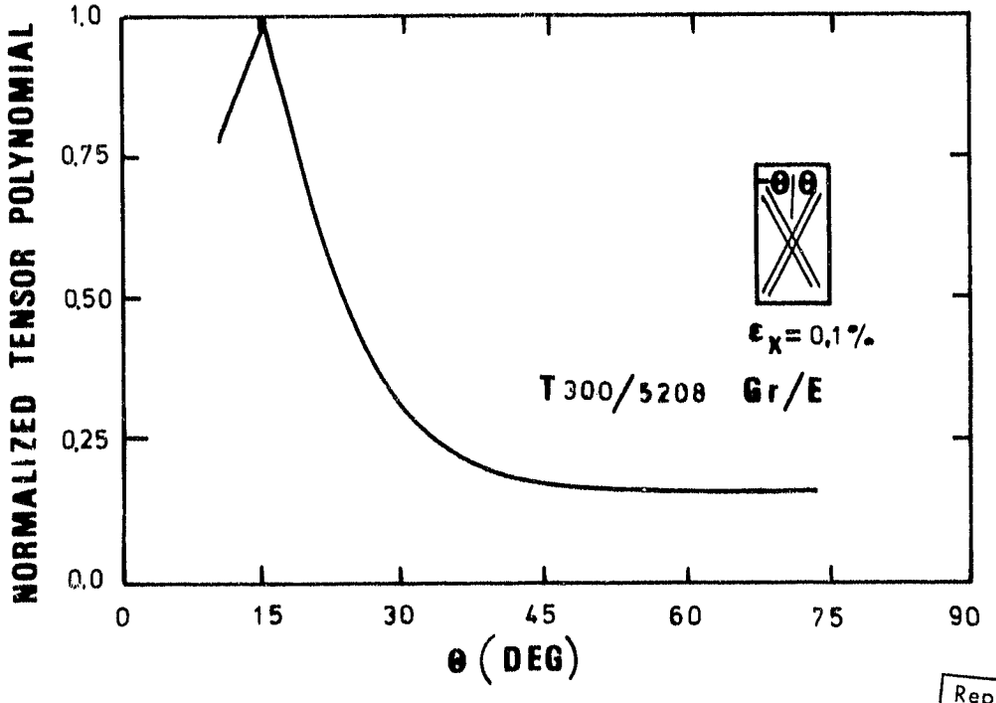

Figure 5 - Maximum tensor polynomial values for $[\pm \theta]_s$ laminates

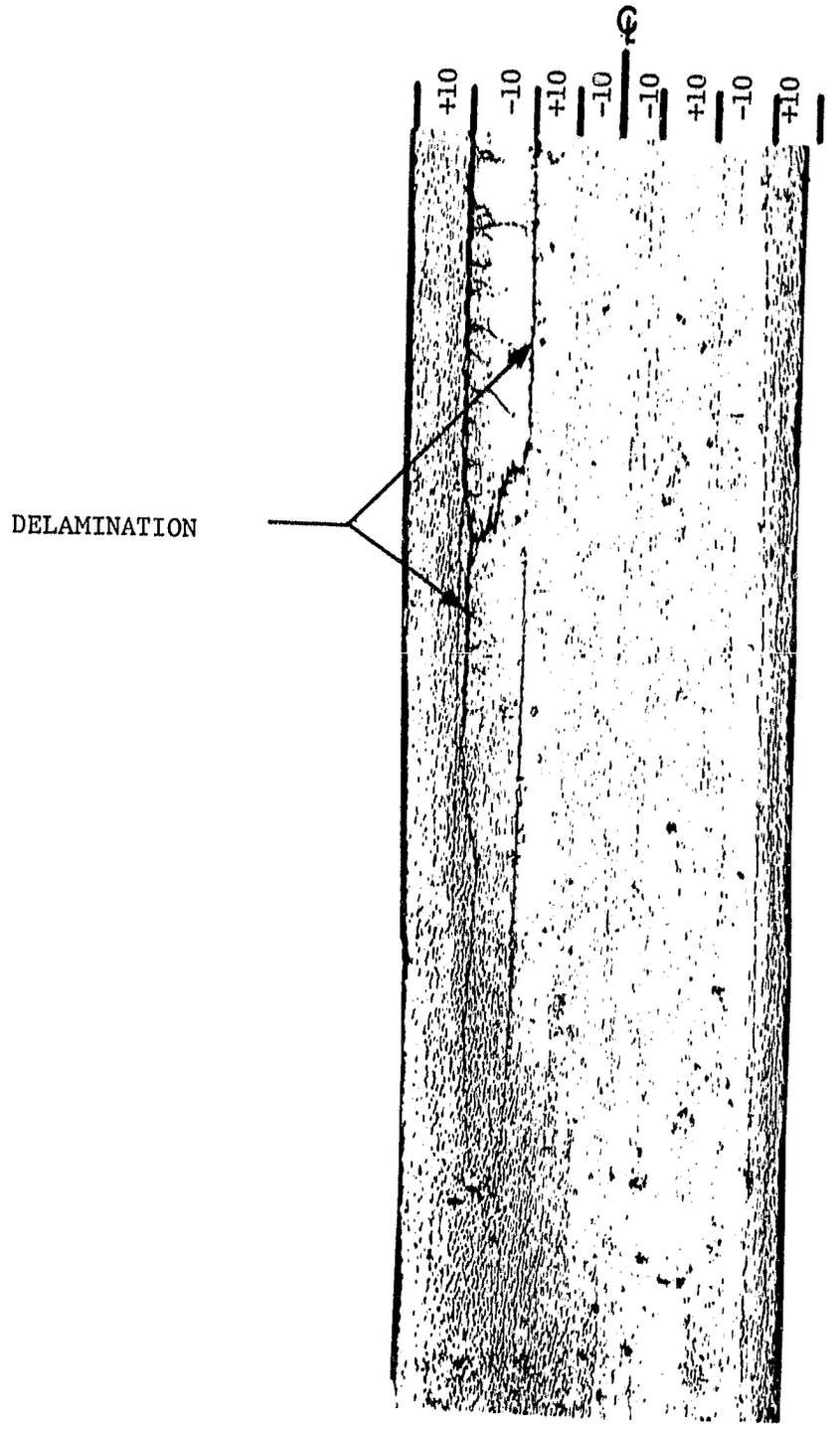

Figure 6 : EDGE DAMAGE IN A $[(\pm 10)_2]_s$ CELION 6000/PMR-15 GRAPHITE-POLYIMIDE LAMINATE AT 99% OF ULTIMATE STRAIN

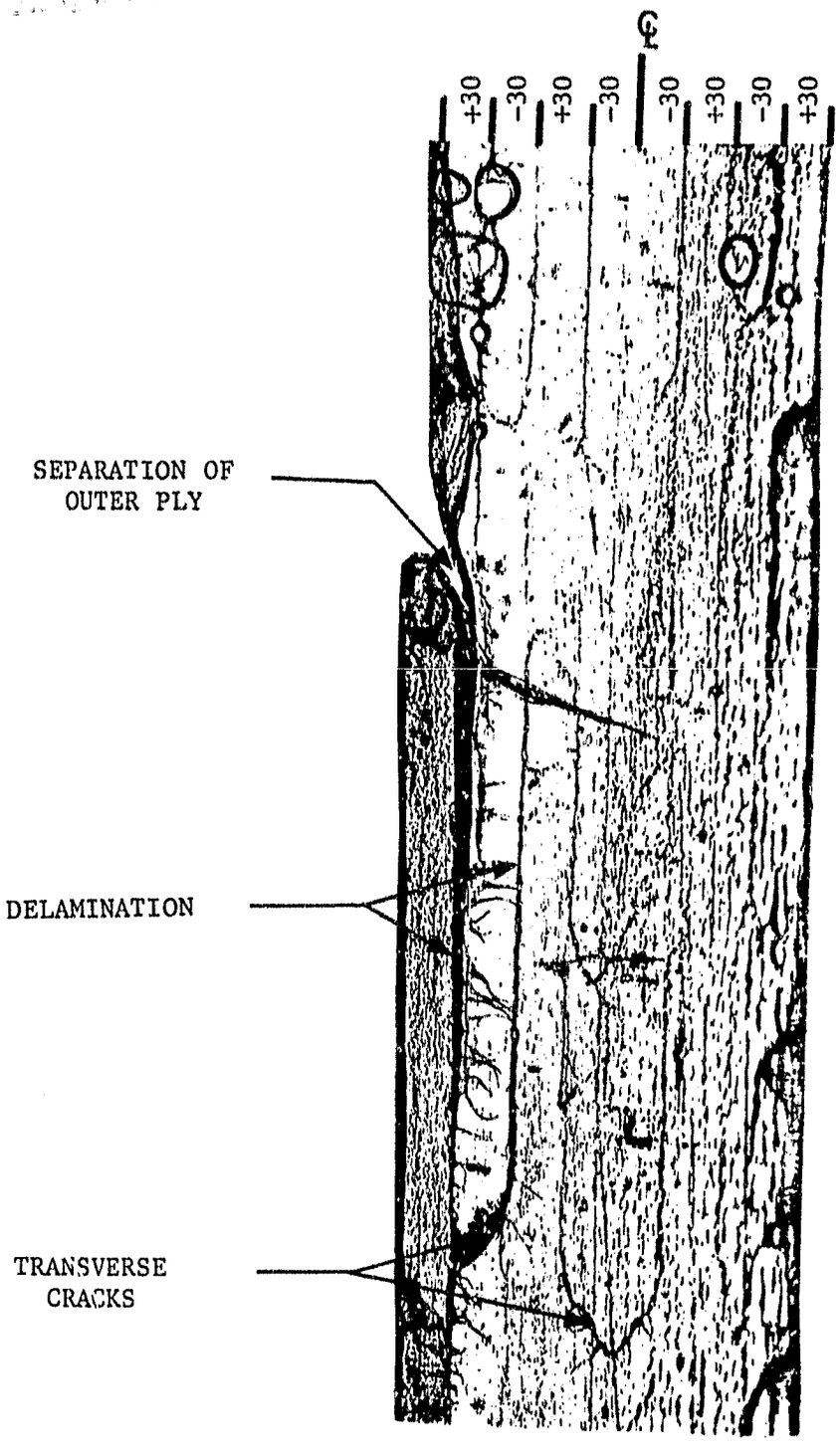

Figure 7 : EDGE DAMAGE IN A $[(\pm 30)_2]_s$ CELION 6000/PMR-15 GRAPHITE-POLYIMIDE LAMINATE AT 99% OF ULTIMATE STRAIN

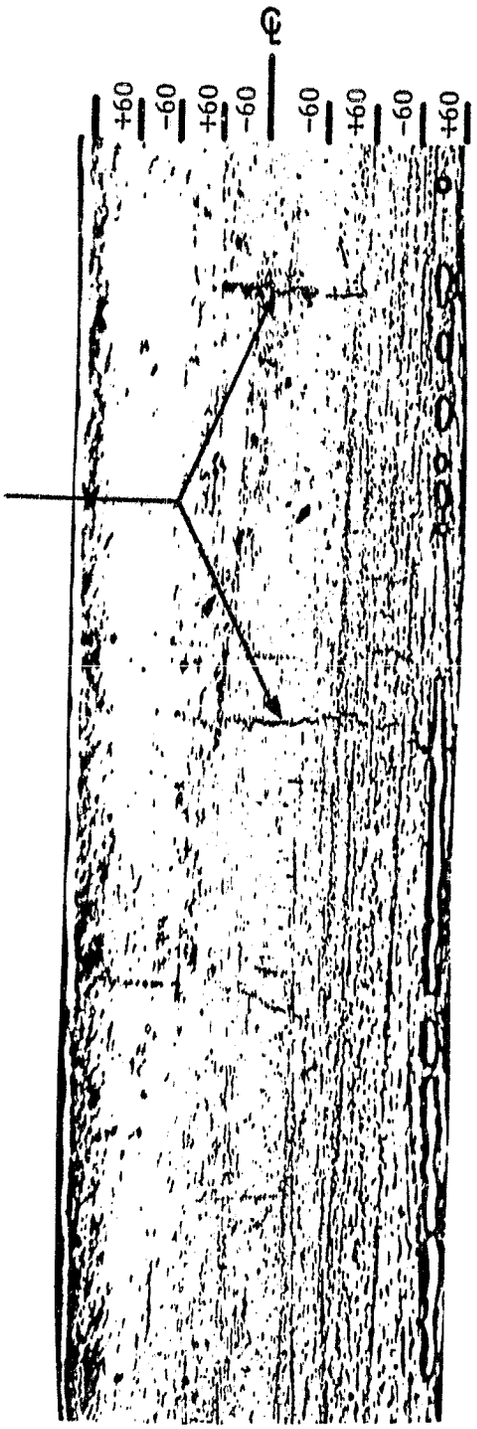

Figure 8 : EDGE DAMAGE IN A $[(\pm 60)_2]_s$ CELION 6000/PMR-15 GRAPHITE-POLYIMIDE LAMINATE AT 99% OF ULTIMATE STRAIN

Strength Hierarchy	Laminate stress σ_y (KSI)	Laminate	Interface Moment $\frac{\text{in - lb}}{\text{in}}$	Finite Element Maximum stresses (KSI)
1	-26.5 → 13.5 ← -0.5 → 13.5 ←	90 / 45 / 0 / -45	-0.33 / -0.83 / -1.16 / -1.33	σ_z = -6.8 τ_{zx} = -6.9
2	-0.5 → 13.5 ← -26.5 → 13.5 ←	0 / -45 / 90 / 45	-0.01 / 0.15 / 0.15 / -0.02	σ_z = 6.2 τ_{zx} = 6.6
3	13.5 ← -26.5 → -0.5 → 13.5 ←	45 / 90 / 0 / -45	0.17 / 0.17 / -0.16 / -0.33	σ_z = 6.6 τ_{zx} = 5.9
4	13.5 ← -26.5 → 13.5 ← -0.5 →	45 / 90 / -45 / 0	0.17 / 0.17 / 0.02 / 0.02	σ_z = 6.9 τ_{zx} = -6.5
5	13.5 ← -0.5 → -26.5 → 13.5 ←	45 / 0 / 90 / -45	0.17 / 0.50 / 0.50 / 0.33	σ_z = 7.6 τ_{zx} = -5.8
6	13.5 ← -0.5 → 13.5 ← -26.5 →	45 / 0 / -45 / 90	0.17 / 0.50 / 0.99 / 1.33	σ_z = 10.4 τ_{zx} = -6.0

○ - Maximum $|\tau_{zx}|$ T300/5208 Graphite-Epoxy

□ - Maximum $|\sigma_z|$ ε_x = 0.5%

Table 1 : Strength hierarchy for interspersed ±45° layers.

Strength Hierarchy	Laminate stress σ_y (KSI)	Laminate	Interface Moment $\left(\frac{in - lb}{in}\right)$	Finite Element Maximum stresses (KSI)
7	-26.5 → 90 -0.5 → 0 13.5 ← -45 13.5 ← 45		-0.33 -1.00 -1.50 -1.67	σ_z = -8.2 τ_{zx} = 9.0
8	-26.5 → 90 13.5 ← 45 13.5 ← -45 -0.5 → 0		-0.33 -0.82 -0.98 -0.98	σ_z = -7.4 τ_{zx} = -9.2
9	-0.5 → 0 -26.5 → 90 13.5 ← 45 13.5 ← -45		-0.01 -0.34 -0.85 -1.02	σ_z = -7.6 τ_{zx} = -9.2
10	-0.5 → 0 13.5 ← 45 13.5 ← -45 -26.5 → 90		-0.01 0.15 0.65 0.98	σ_z = 10.0 τ_{zx} = -8.3
11	13.5 ← 45 13.5 ← -45 -26.5 → 90 -0.5 → 0		0.17 0.67 1.02 1.02	σ_z = 9.0 τ_{zx} = -7.7
12	13.5 ← 45 13.5 ← -45 -0.5 → 0 -26.5 → 90		0.17 0.67 1.34 1.67	σ_z = 10.9 τ_{zx} = -7.2

○ Maximum $|\tau_{zx}|$ T300/5208 Graphite/Epoxy

□ Maximum $|\sigma_z|$ ϵ_x = 0.5%

Table 2 : Strength hierarchy for adjacent ± 45° layers.